Ge nanostructures grown by self-assembly; influence of substrate orientation

2002 J. Phys.: Condens. Matter 14 8235

(http://iopscience.iop.org/0953-8984/14/35/304)

INSTITUTE OF PHYSICS PUBLISHING JOURNAL OF PHYSICS: CONDENSED MATTER

J. Phys.: Condens. Matter **14** (2002) 8235–8252 PII: S0953-8984(02)31235-9

Ge nanostructures grown by self-assembly; influence of substrate orientation

L Vescan

Institut für Schichten und Grenzflächen (ISG), Forschungszentrum Jülich GmbH, D-52425 Jülich, Germany

E-mail: l.vescan@fz-juelich.de

Received 26 November 2001
Published 22 August 2002
Online at stacks.iop.org/JPhysCM/14/8235

Abstract

The present paper discusses structural and optical properties of self-assembled random and non-random Ge dots on finite-area mesa substrates with facets with high-index orientation under conditions of strong surface diffusion. The island formation on the (001) top surface of the mesas was found to be different if other crystallographic planes are within the diffusion length. The growth on mesas is dominated initially by preferential nucleation of ordered islands on $\{hkl\}$ facets and later by random nucleation of islands of more uniform sizes on the (001) top surface. The shape of ordered islands is influenced by the anisotropic properties of high-index surfaces. A transition of ordered islands from trapezoid-based to elongated domes with high aspect ratio was identified, with a mono-modal distribution in each stage of growth. We discuss these features in terms of strong island–island interaction and fast surface diffusion. The relevant change of the optical properties of ordered islands with respect to the random (001) case is the narrowing of photoluminescence peaks.

1. Introduction

The strain and surface energy of a film/substrate system determine the film energy, leading for Ge/Si to a Stranski–Krastanov growth mode (Bauer 1958). While equilibrium theories explain well the key mechanisms (Tersoff 1991, Tersoff and Tromp 1993, Gray *et al* 1995, Spencer and Tersoff 1997, Daruka *et al* 1999), the interpretation of the experiments is often complicated because equilibrium and non-equilibrium phenomena usually coexist during growth. A typical example is the island growth at temperatures above ∼500 °C when the process of elastic strain relaxation is affected by intermixing (Carlino *et al* 1996, Chaparro *et al* 1999, Capellini *et al* 2001). The strain energy which accumulates in the growing film favours intermixing; therefore, during deposition of pure Ge the Si content in the wetting layer and in the island increases. The island alloying leads in turn to an increase of the island size (both for pyramidal and

dome-shaped islands). Another example is the observation that the thickness of the wetting layer increases with temperature (Gossmann and Fisanick 1990). The increase observed for pure Ge deposition is from 3.10 to 3.16 ML in the temperature range 200–550 °C. This was explained by the existence of an additional uniform layer at non-zero temperature. However, we believe that this increase is again an intermixing effect. It is known that intermixing during growth increases the critical thickness for 2D–3D transition (h_{SK}) as $1/x^4$, where x is the Ge content (Osten *et al* 1994). Assuming for $x = 1$, $h_{SK} = 3.10$ ML, then from $h_{SK}(x) = A/x^4$, we obtain $A = 3.10$ ML. Therefore for $h_{SK} = 3.16$ ML, one gets $x = 0.99$, i.e. a Si content of 1%, a value for intermixing which is quite realistic at 550 °C. Strain also governs shape transitions, which leads on Si(001) to bimodal (Kamins *et al* 1997, Ross *et al* 1998) or trimodal distributions (Goryll *et al* 1997).

The structure of islands is affected by mismatch strains and surface stress and in addition by film–substrate interaction (Eaglesham and Cerullo 1990) and surface energy anisotropy. The surface energy depends on crystal orientation and surface reconstruction at the growth temperature.

Here we examine the influence of substrate orientation on the formation, the morphology and the optical properties of islands. In section 2 we give a brief review of previous work on self-assembly on different substrate orientations. The dimensions of these substrates are usually much larger than the surface diffusion length (λ_S) of Ge; we call this case 'infinite area'. In section 3, islanding on finite areas, in particular on (001) mesas, of the order of λ_S is described; in section 4, we examine non-random and preferential nucleation on mesa facets; and finally in section 5, we discuss the photoluminescence (PL) of ordered islands in comparison to that of random islands.

The experimental data presented here are for Ge islands deposited in a low-pressure chemical vapour deposition (LPCVD) system at 0.12 Torr. The Si source is $SiCl_2H_2$, the Ge source is GeH_4 diluted 10% in He and the carrier gas is H_2. The deposition temperature during island growth was 700 °C. Several (001)-oriented patterned and unpatterned wafers were deposited simultaneously. Other deposition and characterization details are given in the references (Vescan *et al* 1992, Apetz *et al* 1995, Goryll *et al* 1997).

2. Ge islands on Si{hkl} substrates of infinite area

Table 1 compares islands deposited on the high-symmetry planes (001), (111), (110) and on the high-index plane (113). The choice of data from the literature was influenced by the experimental data that we want present here, in particular regarding temperature and coverage ranges. We compare data for h_{SK} and for the shape, width, density and intermixing of islands for low coverage (only coherently strained islands). Self-assembly of Ge on Si(001) substrates has been discussed intensively in the literature and overall agreement concerning the value of h_{SK}, island shape and Si interdiffusion exists.

The SK transition of Ge is governed by the mismatch strain given by the difference in lattice constants $\Delta a = a_{\mathrm{Si}} - a_{\mathrm{Ge}}$ and by the surface free energies, γ_{Si} and γ_{Ge} (Bauer 1958). Because $\gamma_{\mathrm{Ge}} < \gamma_{\mathrm{Si}}$ over a large temperature range, the growth proceeds first as a fully strained 2D layer (also known as a wetting layer), followed by nucleation of islands on top of the wetting layer when coverage exceeds h_{SK}. Thus, above h_{SK} any Ge atom deposited in excess forms or attaches to islands. These are, for low coverages, coherently strained. The *elastic* relaxation of the island is enabled by the elastic deformation of the substrate, as observed by Eaglesham and Cerullo (1990) from strain contrast in cross-section TEM samples. The essential participation of the substrate in the relaxation process is supported by theoretical calculations (Christiansen *et al* 1994, Gray *et al* 1995). In the former reference, finite-element calculations showed that

Table 1. Data from the literature for coherently strained Ge islands deposited in the temperature range 600–760 °C on large substrates of different orientations; h_{SK}—critical thickness for the SK transition in ML of pure Ge.

{*hkl*}	T_{epi} (°C)	h_{SK} (ML)	Island shape	Width (nm)	Density (μm^{-2})	Si interdiffusion	Reference
001	600–700	3–5[a]	Square pyramid	80	~ 50		[b]
			and domes	140	~ 5	25–50%	[b]
111	< 627	4	Frustum of a tetrahedron		Low		Voigtländer and Zinner (1993)
111	600–690	4.6	Flat and large	1000	0.6–0.1		Shklyaev *et al* (1999)
111	677	4.5					Walz *et al* (1998)
111	650	4	Small triangle,	200			LeGoues *et al* (1996)
			elongated	1000			
110	760	4		500	0.06		Arai *et al* (1997)
110	700	3.7	Dome	50–160	80		Ferrandis and Vescan (2002)
110	700			200	1		Weil *et al* (1998)
113	700	4.6	Mesa-like, elongated	500	0.03	33%	Zhu *et al* (1999)
113	740	3	Isosceles triangle	1000			Amano *et al* (1998)

[a] Zinke-Allmang and Stoyanov (1990), Gossmann and Fisanick (1990), Sunamura *et al* (1995), Schittenhelm *et al* (1995), Kamins *et al* (1997).
[b] Zinke-Allmang (1999), Capellini *et al* (2001).

at approximately 3.5 times the island height deep into the substrate, there is still a displacement of 0.1 of the maximum displacement.

2.1. Morphology of random islands

The substrate orientation plays a central role in the growth process. {111} is the slowest-growing plane, which is consistent with its lowest surface energy and the associated incorporation difficulty (table 2, Rai-Choudhury and Schroder (1973)). Because of ease of nucleation and high surface energy of the (001) plane, the growth rate of Si on this plane is higher than on {111}. The knowledge of the surface energies is not trivial. The surface reconstruction which influences this physical property depends on temperature and on coverage. For this reason we have chosen for our discussion data determined at a temperature near to that for the data of table 1. Some reasonable trends may be derived from table 2 for Si: {111} exhibits the lowest surface energy, {113} belongs to the group of low-energy surfaces and the value for {110} is surprisingly high (Jacobi 1999). Table 2 shows the following trends for the surface energy: $\gamma_{111} < \gamma_{001} < \gamma_{113} < \gamma_{110}$. For the homoepitaxial growth of Si, the following growth rate relationship exists in the range 700–750 °C: $R_{111} < R_{110} < R_{113} < R_{001}$. Far fewer data are available for Ge on Si {*hkl*}, but we expect similar relationships in spite of the presence of strain. For the growth rate of Ge at 700 °C we observed the relationship $R_{111} < R_{110} < R_{001}$, which is thus similar to the homoepitaxial growth.

In self-assembly, the surface orientation affects the in-island elastic relaxation due to the anisotropy of elastic properties. Self-assembly of III–V on (11*N*) high-index substrates shows a slight increase of h_{SK} with N. This was attributed to the less efficient in-island elastic relaxation for islands grown on high-Miller-index surfaces (Sanguinetti *et al* 1999). We discuss now the substrate orientation in more detail.

Table 2. Comparison of the major Si surfaces. The experimental surface energies were determined at 700 °C and are normalized to the value for the (001) surface (Eaglesham *et al* 1993). The growth rate of Si is normalized to the value for the (001) surface (Vescan *et al* 1998). The numbers of bonds are for an unreconstructed surface.

Crystal plane	Surface energy	Growth rate	Bonds available per atom
001	1.00	1.00	2
113	1.01	0.63	1–2
110	1.05	0.50	1
111	0.90	0.30	1

2.1.1. Ge/Si(001). On the (001) surface each atom has two dangling bonds. A depositing atom can bond to two surface atoms leaving the other two bonds unsatisfied. The easy bonding makes the growth rate on this surface the highest one (table 2).

There is general agreement that $h_{SK}(001) = 3$–5 ML during continuous growth over a large temperature range (table 1). Moreover, even for deposition at room temperature and subsequent annealing at 400 °C, h_{SK} lies within this range (Gossmann and Fisanick 1990). This implies that the inequality $\gamma_{\mathrm{Ge}} < \gamma_{\mathrm{Si}}$ remains valid from 400 °C up to at least 700 °C which in turn signifies that the surface reconstruction does not change remarkably in this temperature range. The relatively large transition range reported (3–5 ML) might be due to the different experimental conditions, leading for instance to different degrees of intermixing in the wetting layer.

Islands on Si(001) are of two types. Initially, there are square-based, single-faceted pyramids with a low aspect ratio and ∼80 nm in size. The later stage in growth involves a shape transition of these small islands to multi-faceted, round domes with a high aspect ratio and 100–180 nm in size (Eaglesham and Cerullo 1990, Capellini *et al* 2001), allowing for a higher degree of elastic strain relaxation (Ross *et al* 1998). For the size of domes a scaling law was found which relates the width, w with the Ge content (i.e. with the strain): $w \sim x^{-2}$ (Dorsch *et al* 1998). The islands change their Ge content during growth from $x = 1$ to lower values, the intermixing being ∼50% at 700 °C (Capellini *et al* 2001).

The in-island strain relaxation depends on island shape: at 600 °C, pyramids relax only 0.5% of their strain, while domes relax 1–2% (Liu *et al* 2000). This experimental observation is in agreement with a theory predicting that elastic relaxation is stronger for islands with larger aspect ratios (Ratsch and Zangwill 1993, Gray *et al* 1995).

2.1.2. Ge/Si{111}. The Si{111} surface has the lowest energy (table 2) due to the fact that three quarters of the crystal binding energy or cohesive energy is involved in the internal bonding of these double-layer units. The depositing atoms can form only one bond to the surface. Addition of one atom causes the creation of three unsatisfied bonds. For this atom to remain bonded, two additional atoms must attach, one to the existing layer as a second-nearest neighbour of the first and one between the first two. Thus, the difficulty of nucleation and the low surface energy of {111} surfaces are responsible for their slow growth and high stability (Rai-Choudhury and Schroder 1973).

The growth of Ge in this case is also of SK type. Initial growth starts with the formation of a wetting layer, with $h_{SK}(111) = 4$–4.5 ML (table 1). The island density is much lower than on (001) and the size is usually large. The shape depends on the direction of steps on the substrate (LeGoues *et al* 1996). For steps parallel to the $\langle 11\overline{2}\rangle$ direction the islands are very long and elongated. This is due to the fact that nucleation is favoured at these steps because

this allows low-energy facets $\{3\bar{1}1\}$ to be formed. The low density implies large diffusion length of the order of several microns, and this is due to the low probability for incorporation. If the steps deviate from the $\langle 11\bar{2}\rangle$ direction the island cannot follow the step since this would introduce high-energy facets. In this case small, triangle-shaped islands form (table 2).

2.1.3. Ge/Si(110). Atoms on $\{110\}$ surfaces are arranged in zigzag chains, each surface atom having one incomplete bond. The first deposited atom to start the formation of a new layer makes only one bond to the existing surface, creating three dangling bonds. A second atom is needed to bond the first adatom to the underlying surface. It bonds to the parallel zigzag chain. This makes incorporation difficult, too, as seen from the low growth rate (table 2). However, h_{SK} is ∼4 ML, near to the transition thickness on (001) and (111) surfaces. For size and density there are large discrepancies in the literature (see table 1).

2.1.4. Ge/Si{113}. For this high-index plane we expect to observe an effect of the anisotropic elastic properties, because it possesses the highest shear strain from all orientations (De Caro and Tapfer 1993). The Si$\{113\}$ surface seems to belong to the group of high-index surfaces with a rather small surface energy (Jacobi 1999) and was found to be thermally stable. The surface energy is only slightly higher than the free energy of the Si(001) surface (table 2). The $\{113\}$ plane, being close to the (001) surface, does not encounter great nucleation difficulties and the growth proceeds at a rate slightly under that for (001). Island formation starts at 3–4.6 ML (table 1) and the island size is large with a low density. The high island–island separation of 3 μm indicates, similarly to the case for the $\{111\}$ surface, a strong surface diffusion at 700 °C. The low surface energy is demonstrated by the fact that islands have a $\{113\}$ top surface (Zhu *et al* 1999). The islands are generally elongated, which must be due to the high shear strain, although also isosceles-triangle-shaped islands were observed (Amano *et al* 1998). Intermixing is similar to that on (001) and islands relax up to 35% of their strain.

Summarizing the influence of substrate orientation on self-assembly of Ge/Si $\{hkl\}$: the inequality $\gamma_{\mathrm{Ge}} < \gamma_{\mathrm{Si}}$ is valid for all surfaces discussed here, leading to values for $h_{SK}(hkl)$ which do not differ much from each other; the nucleation of Ge is *random* on all surfaces; the size of islands is influenced by the incorporation rate and by the surface diffusion; i.e. if the temperature is high enough, then adatoms will diffuse many micrometres until they incorporate. This makes islands on $\{111\}$ and $\{110\}$ surfaces larger than on the (001) surface, where incorporation is much easier. Finally, the shape depends on the anisotropic elastic properties of the substrate and the intermixing is strong.

2.1.5. CVD growth rate dependence on strain. Recently we observed an initial non-linear regime of growth of Ge/Si(001) reflecting the evolution of strain during growth of the first 10 ML. The growth rate in homoepitaxy is constant during deposition; however, in heteroepitaxial growth the presence of strain and predeposited species can influence the rate during growth (Fernández *et al* 1996). Figure 1 displays the growth rate evolution at 700 °C for a low flow rate of GeH_4. There is a decrease of five times of the rate from the deposition of 2.8 up to 42 ML. Below h_{SK} (short deposition time and small thickness) the rate is high. This corresponds to the initial stage of growth. The growth rate decreases quickly with growth time and continues to decrease even after the SK transition. The growth rate becomes constant after the plastic relaxation of islands starts.

This variation in deposition rate can be understood if the growth by CVD is analysed. At 700 °C the growth is surface kinetically limited. A simplified picture of the growth chain is: adsorption plus decomposition of GeH_4, surface migration of Ge adatoms, incorporation of

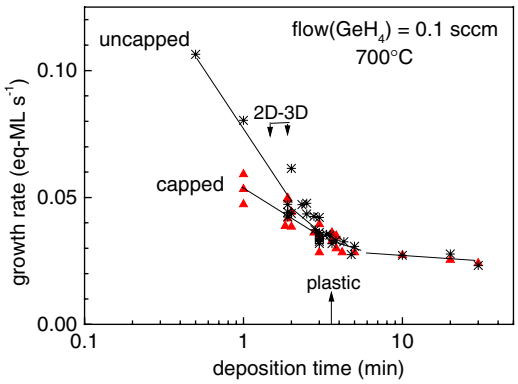

Figure 1. The dependence of the growth rate on deposition time for Ge on Si(001) for flow $(GeH_4) = 0.1$ sccm. Crosses are for uncapped Ge islands and triangles for capped samples. The amount of Ge is expressed in terms of number of equivalent monolayers (eq-ML) of a uniform Ge layer.

Ge on the wetting layer and/or on islands and desorption of the reaction products. Moreover, if the epitaxial layer is lattice mismatched, these phenomena are influenced by strain. The surface migration is known to increase under strain (Gossmann and Fisanick 1990, Sullivan *et al* 1999). Also the adsorption and incorporation are affected by strain. The analysis is complex and will be the subject of a forthcoming paper (Stoica 2002). Here it is important to remark that the growth rate reflects the interface dynamics and the fast surface mass transport during growth. When the strain energy is low (coverage only a few ML), the rate is high; on increasing the number of ML, the strain energy increases and the growth rate decreases due to a decrease of the incorporation rate.

Figure 1 shows also that in the early stage of growth there is a large difference between the growth rates of uncapped and capped Ge. The thickness of capped Ge is systematically lower than for uncapped samples by ∼1 ML. This can be explained as follows: for the growth of cap layers using chlorine-containing gases, the reaction product is HCl. Therefore the etching reaction $Ge + 2HCl \rightarrow GeCl_2 + H_2$ becomes possible as soon as $SiCl_2H_2$ is switched on. Approximately 1 ML Ge will be etched; then etching stops because the overgrowth by Si will be faster. We expect this phenomenon not to occur if SiH_4 is used for capping, because the etching agent is absent and the growth rate is much higher.

2.2. Luminescence of random islands on {hkl} substrates

PL spectroscopy is a helpful tool for understanding size distribution and island microstructure; in particular it can reveal the SK transition. Usually, there are emission peaks which can be without doubt ascribed to islands, but under certain circumstances no island emission is detected, although islands exist as seen by TEM or AFM. This will be discussed in more detail below. We review here some of the results relevant for further discussions.

2.2.1. Photoluminescence of Ge/Si(001). Recently, Goryll *et al* (1999) examined the influence of island size on PL properties. All samples had a thickness of ∼6.4 eq-ML. At high growth rate and small deposition times, a broad distribution was obtained consisting of pyramids and domes. At low growth rate and high deposition time the size distribution was much narrower, mainly domes being present. The PL spectra of all samples revealed island-

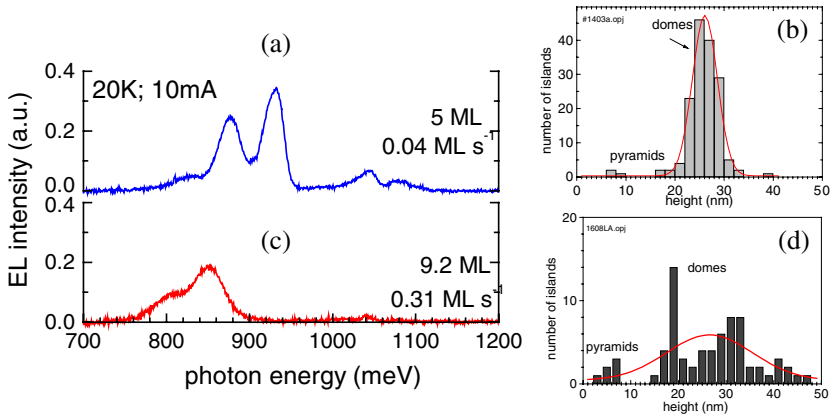

Figure 2. Spectral distribution of electroluminescence for two samples deposited at 700 °C and the height distribution of islands on uncapped samples grown under the same conditions. (a) and (b) are for samples with two stacked island layers, $d_{\mathrm{Ge}} = 5$ eq-ML, $R_{\mathrm{Ge}} = 0.04$ eq-ML s^{-1} and Si spacer thickness of 6 nm; (c) and (d) are for samples with single-island layers, $d_{\mathrm{Ge}} = 9.2$ eq-ML, $R_{\mathrm{Ge}} = 0.31$ eq-ML s^{-1}.

related peaks; however it was obvious that the presence of pyramids broadens the NP and TO peaks. In samples with higher coverages, in which plastic relaxation of domes occurred, the PL peaks broadened even more until the NP and TO peaks could not be separated any longer; this was accompanied by a further decrease of the intensity (Vescan *et al* 2000b). The reason for the weak emission of pyramids could be the presence of Ge–Ge p-type bonds for which the dipole transition probability is zero (Miyao *et al* 1998). For domes with dislocations, the reason for the reduction in PL emission is similar to that for the disappearance of band-to-band PL in thick SiGe layers or in SiGe quantum wells (Hartmann *et al* 1993), i.e. dislocations have dangling bonds which act as deep levels trapping the excitons. Concluding, a narrow distribution of domes is necessary for intense and well resolved island PL spectra.

There are different experimental and theoretical approaches proposed for achieving a narrower size distribution. The theory of Shchukin *et al* (1995) predicts conditions for surface energy and elastic interaction between islands which allow the avoidance of Ostwald ripening corresponding to the formation of a stable array of islands. The experimental approach discussed above involves deposition at low growth rate and coverages of 7–10 ML allowing for the disappearance of pyramids and narrowing of dome size. Vertical stacking with spacers thin enough to induce vertical ordering leads also to narrower size distributions (Tersoff *et al* 1996). Here we want to show the effect of size distribution on the lineshape of emission of p–i–n diodes. Narrowing was achieved by stacking two layers. Figures 2(a) and (b) correspond to samples with a narrow size distribution with two stacked layers. The EL peaks are well resolved, in contrast to the case for the samples in figures 2(c) and (d) which are single-island layers with a much broader size distribution. It is noteworthy that the NP and TO peaks of the sample in figure 2(a) lie at higher energy than those in the lower spectra. This is attributed to the fact that domes are more elastically relaxed due to the vertical interaction. The lateral ordering along mesa edges is another approach and will be discussed in more detail in section 4.

2.2.2. Photoluminescence of Ge/Si(110). The lineshape of the PL of the islands is a broad peak lying at ∼850 meV (Arai *et al* 1997, Ferrandis and Vescan 2002). The interpretation is not straightforward, as the energetic position is determined by a combination of at least

three parameters: strain, Ge content and island height. Most of the published PL data for Ge/Si(001) deposited above ∼600 °C show this energetic position. So far only a qualitative conclusion can be reached: that the combined effects of strain, intermixing and size are similar for the two surfaces. Moreover, the intensity is comparable with the emission of domes on Si(001); however, the difference is that for the {110} surface the NP and TO peaks cannot be resolved. Such broad peaks are typical for Ge islands on Si(001) when the distribution is bimodal (Vescan *et al* 2000), thus reflecting a broad distribution in island height and a non-uniform microstructure.

2.2.3. Photoluminescence of Ge/Si{113}. No emission was detected from Ge islands on these substrates, only emission from the wetting layer (Amano *et al* 1998, Zhu *et al* 1999). It is not obvious why islands on {113} do not emit light. Even very thin 2D Ge layers show intense PL peaks. The absence of emission from islands on {113} substrates could be due to the fact that, being quite large, the islands are plastically relaxed and in this case dislocations trap all excitons.

Since PL depends strongly on the microstructure of the islands, we can conclude at this point that the influence of the substrate orientation on the optical emission is strong. However, the understanding of the PL properties is far from being complete.

3. Ge islands on finite-area Si(001)

Mesas are non-planar substrates with several crystallographic planes. A non-random island distribution is expected when the area available for deposition has a lateral dimension of the order of the diffusion length of the adatoms. Moreover, if other crystallographic planes are present at the edges of the (001) top surface, islanding on these planes is expected to influence the islanding on the (001) plane. We have seen that self-assembly on {111}, {110} and {113} planes is quite different from that on (001) substrates. However, for the present discussion it is irrelevant why islands nucleate preferentially not on the (001) plane; only the consequence is important, namely, there will be *less* material available for nucleation on the (001) part.

3.1. Surface migration of Ge on the Ge(001) wetting layer

We do not know yet which kind of reconstruction the Si(001) surface has under CVD conditions. But if the reconstruction is (2×1), then the dimers run along ⟨110⟩ directions and the motion is anisotropic with the fast-diffusion direction being along the dimer rows, as under high-vacuum conditions (Mo *et al* 1992). The experiments carried out to evaluate the diffusion length, described below, were performed on square and rectangular (001) mesas with edges parallel to ⟨100⟩; i.e. the dimers on the (001) top surface should run diagonally on the mesas. We therefore expect equal nucleation contributions on all four facets.

Surface diffusion will obviously play a central role in this case. In particular, the strain should increase the diffusion of Ge on Ge as compared to diffusion of Ge on Si (Gossmann and Fisanick 1990). Figure 3 illustrates the coverage dependence of the density of random islands on the (001) part of the mesas. For the lowest coverage, the smallest island-free area was $100 \times 100\ \mu\text{m}^2$; therefore the diffusion length must be of the order of $100\ \mu$m. This value is much larger than the island size and the inter-island distance (∼400 nm) on infinite areas. The large diffusion length found here demonstrates also that the surface is free of species, such as carbon or other impurities, which could reduce the surface diffusion. The atomic hydrogen which is always present during the decomposition of GeH_4 obviously does not passivate the surface. Therefore, we can conclude that the surface diffusion (λ_S) is not the limiting factor

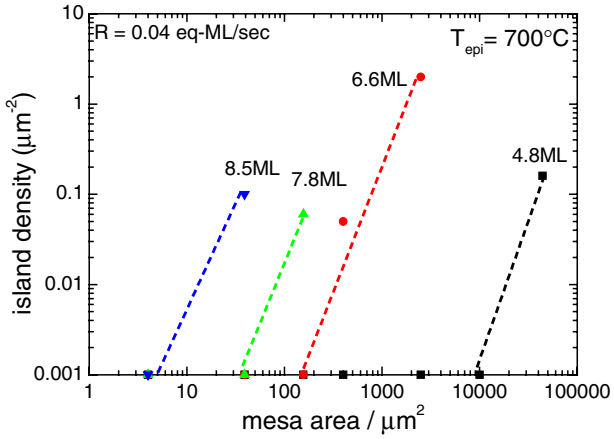

Figure 3. The density of random islands on the (001) plateau of mesas. On large areas, $h_{SK}(001) = 3$–5 ML. $R_{\mathrm{Ge}} = 0.03$–0.04 eq-ML s^{-1} (Vescan *et al* 2000b).

for island nucleation on Si(001). We use Einstein's formula $\lambda_S = (Dt)^{0.5}$ and $D = \nu a^2/4$, where ν is the hopping rate, a is the hopping distance, t is the time taken to deposit 1 eq-ML. The hopping rate is given by $\nu = \nu_0 \exp(-E_{diff}/kT)$; $\nu_0 = kT/2h$, h is the Planck constant. With $a \sim 0.4$ nm, $T = 973$ K, $t \sim 30$ s and $\lambda_S > 100$ μm we find for the activation energy for surface diffusion of Ge on coherently strained Ge an upper limit of $E_{diff} \leqslant 0.6$ eV. This value has to be compared with the value of 0.70 eV determined under ultrahigh-vacuum CVD conditions (Sullivan *et al* 1999) and the value of 0.84 eV found by Zinke-Allmang and Stoyanov (1990), both values being for Ge on strained Ge. The activation energy for surface diffusion of Si on Si is 0.67 eV (Mo *et al* 1992).

3.2. Island size distribution on Si(001) mesas

To find out the influence of mesa area on size distribution, growth of Ge was performed with a relatively high growth rate (0.3 ML s^{-1}), to obtain bimodality on large areas (Vescan *et al* 2000c). An interesting result is that the reduction of the deposited area has a beneficial effect on the size distribution. This is clearly demonstrated in figure 4 where we compare large-area and 50×50 μm^{-2} mesas. While on large areas the diameter and height distributions are broad, on the 50×50 μm^{-2} mesas the distributions are much narrower. For instance, big islands of height 31–48 nm and diameter 180–230 nm seen on large areas do not form any longer on the small mesas. The 50×50 μm^{-2} mesas have a higher dome density, a smaller dome size and a better uniformity than the large areas. This partial suppression of Ostwald ripening might be due to the stronger island–island interaction on areas smaller than λ_S^2.

4. Lateral ordering of Ge/Si{hkl}

When Ge is deposited on Si mesas, ordered nucleation occurs along the edges, beside the random nucleation on the (001) part (Kamins *et al* 1997, Jin *et al* 1999, Vescan *et al* 2000a). Ordering occurs for both side-wall orientations, but in most experiments islands are observed to order on the (001) top of the mesa (see table 3). For mesas parallel to ⟨100⟩ the ordering occurs in some experiments on high-index planes near the edge to the {110} facets. The results presented in table 3 were obtained in different epitaxial systems and for a total pressure

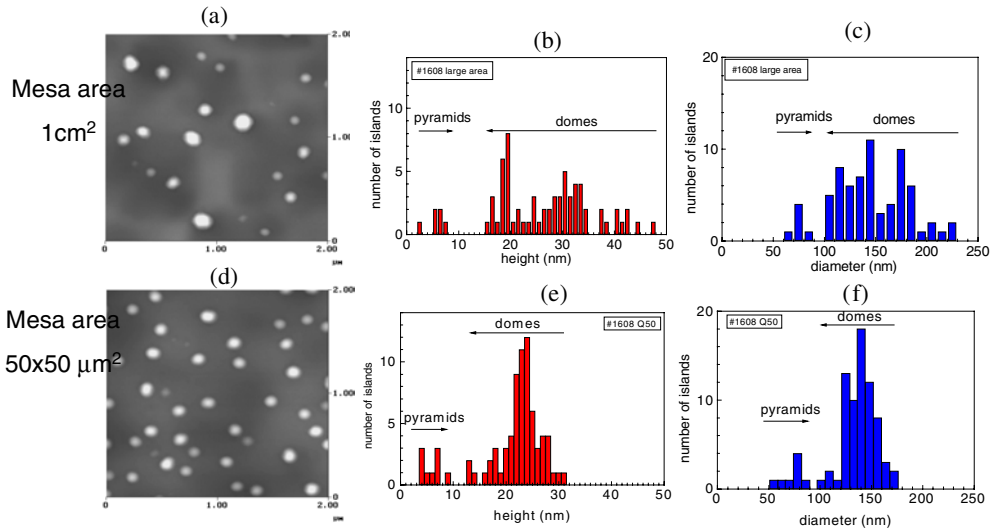

Figure 4. AFM pictures and island size distribution for a large-area part of 1 cm^2 ((a)–(c)) and for a 50×50 μm^{-2} mesa ((d)–(f)) on the same wafer. The scan area of the AFM pictures is 2×2 μm^{-2} and the substrate orientation is Si(001); $d_{Ge} = 6.2$ eq-ML, $R_{Ge} = 0.20$ eq-ML s^{-1} (Vescan *et al* 2000).

Table 3. Data from the literature for laterally ordered Ge islands on Si mesas.

T_{epi} (°C)	Ordering along	Plane for ordering	Linear density (μm)	System, pressure (Torr)	Island width (nm)	References
600	⟨100⟩	(001)	10	RTCVD, 20	75	Kamins *et al* (1997)
630	⟨110⟩	(001)	8	GSMBE, 10^{-5}	80	Jin *et al* (1999)
700	⟨110⟩	(001)		GSMBE, 10^{-5}		Kim *et al* (1999)
700	⟨100⟩	{12 1 0}	∼7	LPCVD, 0.12	90–160	Vescan *et al* (1998, 2000a)

ranging from atmospheric pressure down to the molecular regime, but the linear density and size of ordered islands do not seem to be influenced by this parameter. A strong influence of the orientation of the mesa facets is expected to be present; however, a systematic study has still to be done.

In our experiments the ordering of islands was studied on Si mesas grown at 800 °C on Si(001). At this temperature only the {12 1 0} and {110} facets develop on long mesas oriented parallel to ⟨100⟩ directions, while along ⟨110⟩ directions the {113} form and under certain conditions also the {119} facets. The self-assembly on mesas is randomly on the (001) part and ordered along the edges. Ge islands order on the {12 1 0} facets in single, dense rows near the edge to the {110} facets. The ordered rows are as long as the mesa, e.g. ∼1000 μm long. In the following we shall discuss some features of ordered islands on the high-index {12 1 0} facets.

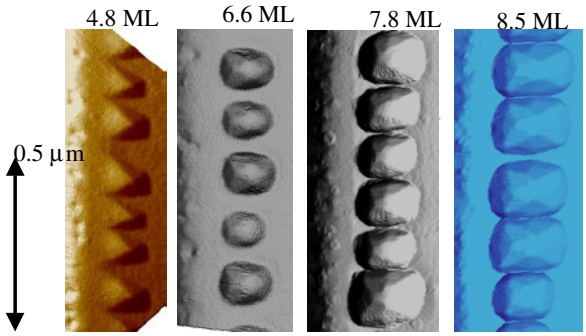

Figure 5. Shapes of ordered islands on {12 1 0} facets of 30 μm long Si mesa stripes; $R_{Ge} = 0.03$–0.04 eq-ML s^{-1}. The average thickness of Ge evaluated on unpatterned areas is: 4.8, 6.6, 7.8 and 8.5 eq-ML.

4.1. Shape transition of ordered islands on {12 1 0} facets

At the initial stage of growth the ordered islands have an irregular shape, *trapezoid*-based with four shallow facets, the angle being ∼10°, as displayed in the AFM pictures of figure 5 and the schematic diagrams of figure 6. The parallel sides of the trapezoidal island are parallel to the mesa edge; the long sides almost touch each other, corresponding to an inter-island distance of ∼10 nm. On increasing the coverage from 4.8 to 6.6 ML the shape changes. The islands resemble now *elongated domes* with a high aspect ratio, the long sides having developed steeper facets (∼40°). The increase of the inter-island distance up to ∼70 nm could be due to a strong exchange of adatoms between islands in the row or due to atom detachment from the island base and migration to the top of the island. Further increase of the coverage increases the island size; thus the inter-island distance decreases again to ∼10 nm. The increase of size of domes caused by further increasing the coverage will slow down (self-limiting growth) and simultaneously nucleation on the (001) part of the mesa occurs. The elongated shape is the result of the surface energy anisotropy of the high-index plane (Zhang 1999).

It is noteworthy that ordered islands have a *mono-modal* distribution on all long mesas in all stages of growth. This seems not to be related to the side-wall orientation; it occurs for islands ordered along ⟨110⟩ directions too (Jin *et al* 1999). The single shape must be related to the strong island–island interaction, as the inter-island distance is much smaller than the island size from the beginning of the SK transition.

The *periodicity* is far from perfect, as seen in figures 5 and 7. Some ordered islands are quite near to each other, others quite far apart, as if an island was missing in between. The deviation from a perfect periodicity could be partly due to the undulations of the facets, as a result of misorientation during the lithography. Periodicity is the result of the island–island repulsion. If the repulsion were below a certain value, as for SiGe with lower Ge content, we would expect islands to form without spacing; thus a wire would form. This was indeed observed for $Si_{0.70}Ge_{0.30}$/Si(001) (Vescan *et al* 1997). However, for pure Ge deposition the distortion of the substrate is high (Eaglesham and Cerullo 1990), leading to a significant island–island repulsion through the substrate, and therefore to localized islands. There is a competition between a lower energy barrier for nucleation on the edges and the repulsive forces between the ordered islands through the substrates, resulting in an inter-island distance of the ordered islands of ∼10 nm, as compared to ∼200 nm for random islands on Si(001).

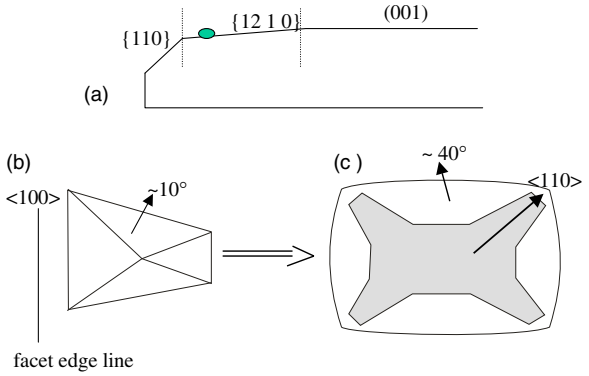

Figure 6. Schematic diagrams of the shape transition of the ordered islands. (a) A cross-section of a mesa with one island on a {12 1 0} facet, (b) the initial stage of growth and (c) a later stage of growth.

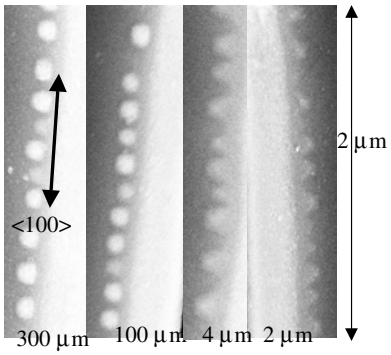

Figure 7. SEM micrographs of uncapped islands on {12 1 0} facets of Si mesas oriented along ⟨100⟩ directions of width: 2, 4, 100 and 300 μm. The coverage on unpatterned areas is 5 eq-ML. The SEM pictures were obtained for non-tilted samples (H P Bochem).

4.2. Size distribution of ordered islands

The size distribution was analysed quantitatively on a series of long mesas of width varying between 1.6 to 300 μm deposited in one run (Vescan and Stoica 2002). Growth conditions were chosen to allow, on a large area, the formation of a bimodal distribution of islands ($\sim$0.6 domes μm^{-2} + $\sim$1.9 pyramids μm^{-2}).

Figure 7 represents SEM pictures of uncapped islands on mesas of width 2, 4, 100 and 300 μm deposited in *one run*. The linear density of islands does not change significantly with stripe width. It is 5.5 ± 0.5 μm^{-1} as displayed in figure 8. However, a variation of the contrast of islands in figure 7 can be observed and this is due to the variation of island height, consistent with the AFM investigations shown in figure 5 where *several* epitaxial growths were performed with decreasing coverage on mesas with the same width. For the narrowest mesa the islands are very shallow, with an aspect ratio of 0.04, as shown in figure 9. On larger mesas the ordered islands have a larger size, being quite 'balled up' with an aspect ratio of $\sim$0.19. While the linear density of islands remains constant within 10%, the island height increases from 6 to 34 nm. Here the variation of island shape, i.e. size, on the same wafer is the result of the decrease of coverage per unit mesa area with decreasing mesa size. This is due to the lower

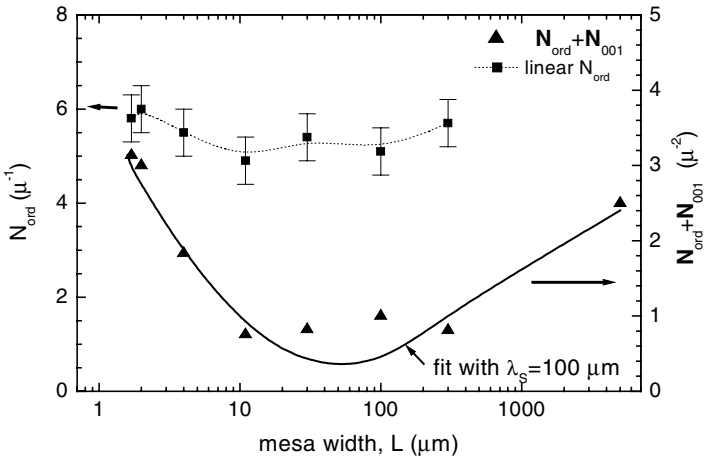

Figure 8. The linear density of ordered islands on {12 1 0} facets and the areal density of ordered plus random islands on (001) parts of long mesas (the sample of figure 7). The continuous curve is the total areal density of islands calculated assuming a diffusion length of Ge on Ge of 100 μm (Stoica 2001).

growth rate on facets. The effect of lower growth rate of Ge on $\{hk0\}$ planes is most evident for mesas with only facets; in this particular case these are mesas $\leqslant 4$ μm. While on the 2 μm stripes the shape is trapezoidal, on all larger stripes the islands are domes. It is remarkable that on all mesas, the ordered island distribution is *mono-modal* independently of the shape, in agreement with the result shown in figure 5.

Figure 8 displays in addition the mesa width dependence of the total areal density of islands. The density was evaluated on an area of 1 mm^2 with arrays of long mesas of different widths. Mesas narrower than 11 μm have only ordered islands. While *the facet width is the same* on all long mesas, the contribution of facets to the total area increases with decreasing width, since their total length increases while the contribution of the (001) top plane decreases. The facet width depends on the buffer thickness and is here $\sim$1.6 μm. The continuous line is a calculation (Stoica 2001) of the total areal density using the equation

$$N(L) = \frac{2N_{ord} + LN_{001}(L)}{L + L_{ox}},$$

where N_{ord} is the linear density of ordered islands, N_{001} is the average areal density of random islands on the (001) part, L is the width of the mesa, L_{ox} is the width of the oxide stripes separating the mesas. To calculate N_{001} we assume that the density of random islands is zero near the mesa edges, maximum in the centre and that it decays exponentially with the distance x from the centre to the edges:

$$N_{001}(x) = N_{001}^{\infty}\left(1 - \exp\left(-\frac{L/2 - x}{\lambda_S}\right)\right)\left(1 - \exp\left(-\frac{L/2 + x}{\lambda_S}\right)\right).$$

The average density on a mesa of width L is given by

$$N_{001} = \frac{1}{L}\int_{-L/2}^{L/2} N_{001}(x)\,\mathrm{d}x = N_{001}^{\infty}\left[1 + \mathrm{e}^{-L/\lambda_S} - 2\frac{\lambda_S}{L}(1 - \mathrm{e}^{-L/\lambda_S})\right].$$

With equations (1) and (3) we obtained the continuous line in figure 8, using for the island density on large areas the experimental values $N_{001}^{\infty} = 2.5$ μm^{-2} and $N_{ord} = 5.5$ μm^{-1} (see above). The best fit with the experimental curve in figure 8 was obtained with $\lambda_S = 100$ μm

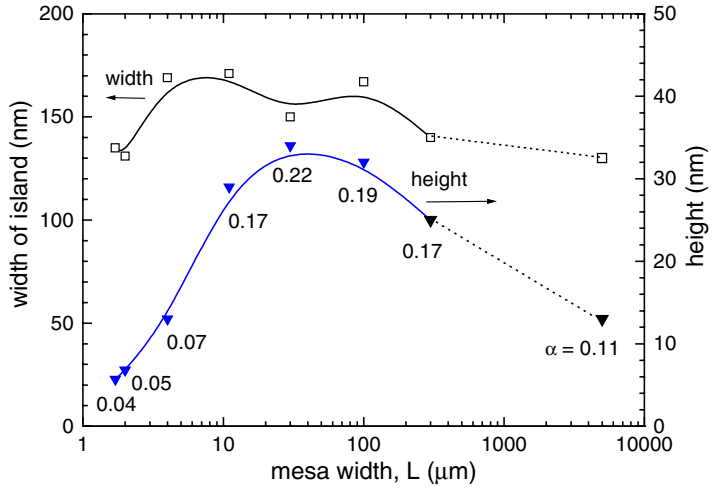

Figure 9. Width and height of uncapped ordered islands on {12 1 0} facets as functions of mesa width measured by AFM for the samples of figure 8; the point at 5000 μm corresponds to the unpatterned area. α is the aspect ratio (height/width), $d_{Ge} = 5$ eq-ML, $R_{Ge} = 0.043$ eq-ML s^{-1}.

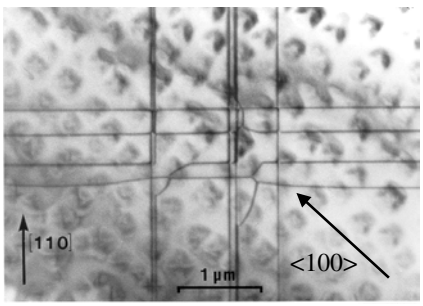

Figure 10. A plan-view TEM of a sample with $Si_{0.70}Ge_{0.30}$ quantum well islands deposited on a plastically relaxed thick buffer; the misfit dislocation lines run along ⟨110⟩ directions while some of the islands order along ⟨100⟩ directions (Vescan *et al* 1992).

(see section 3). This demonstrates again that the surface diffusion length of Ge at 700 °C is extremely long.

4.3. Mechanism for ordering

We have seen that islands form preferentially on facets; in the present study the ordering on facets of the (100) zone will be considered. One possible mechanisms for ordering along ⟨100⟩ directions is that these soft directions allow an easier elastic relaxation of strain than other directions (Shchukin *et al* 1995). For low strain, in particular for $Si_{1-x}Ge_x$ with $x < 0.3$, *short chains* of islands along ⟨100⟩ directions were observed on infinitely large Si(001) surfaces under conditions of fast surface diffusion: by LPCVD at 700 °C (Vescan *et al* 1992), by MBE at 760 °C (Floro *et al* 1997) and by LPE (Schmidbauer *et al* 1998, Christiansen *et al* 1999). One example is illustrated in figure 10 showing a plan-view TEM of ten stacks of vertically correlated islands with $x = 0.30$ on a large-area Si(001) substrate. A clear tendency for ordering along ⟨100⟩ directions can be distinguished (Vescan *et al* 1992).

The ordered islands on mesa facets described in the previous sections are indeed aligned along ⟨100⟩ directions—however, only on facets and in single rows—while no ordered chains on unpatterned regions of the wafer are present. Therefore, the possibility of a 'soft direction mechanism' can be excluded. It is noteworthy that these rows are as long as the mesa edge, so they can be millimetres long. A clear difference between the two ordering cases is in the magnitude of the strain: the ordering on unpatterned wafers along soft directions occurs only for lower strain.

Another possible explanation for ordering, which is not necessarily related to the side-wall orientation, is that mesas are non-uniformly strained. The strain field distribution on Si mesas grown by selective epitaxial growth and oriented along ⟨110⟩ directions was determined by micro-Raman spectroscopy (Jin *et al* 1999). The results suggested a tensile strain near the edges of the mesa and a compressive strain at the centre. Jin *et al* concluded that the strain distribution on Si mesas is the driving force for the preferential nucleation of Ge dots along mesa edges. The strain distribution on the Si mesa surface results in gradients in the chemical potential that significantly influence surface diffusion of the adatoms (Gray *et al* 1995). The surface strain energy is an important component of the chemical potential along the surface. A non-uniform chemical potential produces surface diffusion fluxes proportional to the chemical potential gradient. Adatoms will move to regions of low strain (low chemical potential) enhancing collection and sustained growth in these regions. The mesa centre, being compressively strained, rejects the adatoms which will diffuse to the edges, if these are within λ_S. If ordered tensile strained sites are on the edges, ordered nucleation will take place. The nucleation of a single row reflects the existence of a line along which the strain is minimum, ensuring the ordering along a straight line.

While it is obvious that ordering along mesa edges is due to the existence of tensile sites on the mesa facets, the role of island–island interaction must be considered, as inter-island distances in the rows are smaller than the island size. The mono-modal distribution of islands in the ordered rows could be the consequence of island–island repulsion, as was described in the model of Koduwely and Zangwill (1999). However, we still lack the theoretical framework to understand this behaviour.

5. Photoluminescence of ordered islands

We have seen that islands on the (001) top surface are randomly distributed, while on the {12 1 0} facets the islands form approximately periodic rows (Vescan *et al* 2000). Figure 11 displays the spectral distribution of PL of unpatterned and patterned areas of a capped sample. One feature of all spectra is that the NP and TO peaks from islands and from the wetting layer are well resolved and can be clearly distinguished. While the unpatterned area gives information only about the (001) plane, the arrays of long mesas contribute in addition with emission from the $\{h10\}$ facets.

Comparing the spectra for the random and ordered islands, several features are revealed. First, the spectra of ordered islands are better resolved. We observe a decrease of the FWHM from 42 to 33 meV. This is obviously due to the narrower size distribution discussed in the previous sections. Another feature is the higher emission of ordered islands. This is due to the narrower size distribution but in addition it can be related to another feature, the absence of emission from the wetting layer. The reason is that random domes have a high aspect ratio of $\alpha \geqslant 0.11$, which implies partial elastic relaxation of the islands on their top surface, while around the edges they are tensile strained (Gray *et al* 1995). This leads around the island to a higher chemical potential and therefore to a thinner wetting layer. This is equivalent to a potential barrier for holes preventing the diffusion of holes from the wetting layer to the islands;

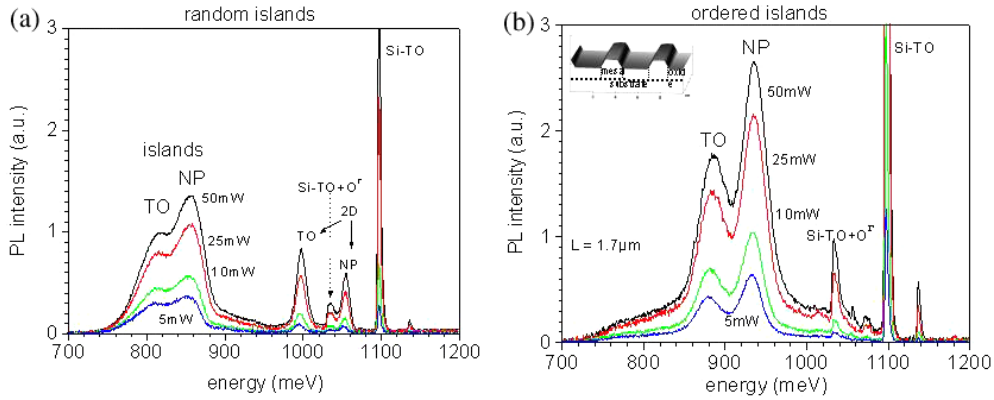

Figure 11. Spectral distributions of PL measured at 20 K: (a) random islands on an unpatterned area and (b) ordered islands on arrays with 5000 μm long mesa stripes; the islands lie on the {12 1 0} facets of the mesas ($d_{\mathrm{Ge}} = 5.6$ eq-ML, $R_{\mathrm{Ge}} = 0.05$ eq-ML s^{-1}). The inset is an AFM 3D scan of two long mesas.

thus PL from both the wetting layer and the islands is observed. In contrast, the ordered flat islands ($\alpha \sim 0.05$) are almost coherently strained; therefore there is no barrier to nucleation around their edge and thus no barrier to diffusion of holes from the wetting layer to the islands, and thus only PL from islands occurs. Finally, the peak positions of island emission lie at higher energy than for the random domes. We expect quantum confinement only due to island height; therefore the shallower ordered islands will emit at higher energy.

6. Conclusions

We have shown that substrate orientation is an important parameter in self-assembly of Ge on Si. For non-planar substrates, such as mesas with facets with different orientations, several effects are observed for self-assembly at 700 °C. On the (001) top mesa surface the ripening of random islands is slowed down, leading to a better uniformity, in contrast to the bimodal distribution on unpatterned (001) areas. The size distribution is dominated by a fast surface diffusion of Ge on strained Ge with an activation energy of 0.6 eV.

On {12 1 0} facets a mono-modal distribution of islands is observed. The islands are periodically ordered with an inter-island distance much smaller than the island size. The ordering on facets seems to be to due the tensile strain of these shallow facets, in contrast to the short-chain ordering along ⟨100⟩ on a large (001) area where under lower strain the ordering is induced by the easier elastic relaxation along the soft directions. While the previous observations of the preferential nucleation on facets have been confirmed, one significant new result is as regards the shape transition of the ordered and closely spaced 3D islands on the high-index surface {12 1 0}. A strong island–island interaction leads to a more uniform distribution of the ordered islands.

We have shown that the analysis of luminescence of self-assembled Ge dots is a helpful tool for understanding the structure and morphology of the dots. The light emission from domes lies around 850–950 meV; however, when pyramids are present the island-related photoluminescence and electroluminescence broaden and even decrease in intensity. The effect of ordering is to narrow the NP and TO peaks, reflecting the narrower distribution in island height. The self-ordering of islands on mesas is very promising as regards realization of large densities of islands with a better homogeneity.

Acknowledgments

We are grateful to T Stoica, B Holländer, M Goryll, A Mück, O Chretien and D Dentel for the fruitful collaboration and to B Voigtländer for helpful discussions.

References

Amano K, Kobayashi M, Ohga A, Hattori T, Usami N and Shiraki Y 1998 *Semicond. Sci. Technol.* **13** 1277
Apetz A, Vescan L, Dieker C and Lüth H 1995 *Appl. Phys. Lett.* **66** 445
Arai J, Ohga A, Hattori T, Usami N and Shiraki Y 1997 *Appl. Phys. Lett.* **71** 785
Bauer E 1958 *Z. Kristallogr.* **110** 372
Capellini G, De Seta M and Evangelisti F 2001 *Appl. Phys. Lett.* **78** 303
Carlino E, Giannini C, Gerardi C, Tapfer L, Mäder K A and von Känel H 1996 *J. Appl. Phys.* **79** 1441
De Caro L and Tapfer L 1993 *Phys. Rev.* B **48** 2298
Chaparro S A, Drucker J, Zhang Y, Chandrasekhar D, McCartney M R and Smith D J 1999 *Phys. Rev. Lett.* **83** 1199
Christiansen S, Albrecht M, Strunk H P and Maier H J 1994 *Appl. Phys. Lett.* **64** 3617
Christiansen S H, Albrecht M, Becker M, Strunk H P and Wawra H 1999 *Epitaxial Growth Principles and Applications (MRS Symp. Proc. vol 570)* ed A L Barabási, M Krishnamurthy, F Liu and T Pearsall (Warrendale, PA: Materials Research Society) p 199
Daruka I, Tersoff J and Barabási A L 1999 *Phys. Rev. Lett.* **82** 2753
Dorsch W, Strunk H P, Wawra H, Wagner G, Groenen J and Carles R 1998 *Appl. Phys. Lett.* **72** 179
Eaglesham D J and Cerullo M 1990 *Phys. Rev. Lett.* **64** 1943
Eaglesham D J, Unterwald F C and Jacobson D C 1993 *Phys. Rev. Lett.* **70** 966
Fernández J M, Hart L, Zhang X M, Xie M H, Zhang J and Joyce B A 1996 *J. Cryst. Growth* **164** 241
Ferrandis P and Vescan L 2002 *Mater. Sci. Eng.* B **89** 171
Floro J A, Chason E, Twesten R D, Hwang R Q and Freunf L B 1997 *Phys. Rev. Lett.* **79** 3946
Goryll M, Vescan L and Lüth H 1999 *Epitaxial Growth-Principles and Applications (MRS Symp. Proc. vol 570)* ed A L Barabási, M Krishnamurti, F Liu and T Pearsall (Warrendale, PA: Materials Research Society) p 205
Goryll M, Vescan L, Schmidt K, Szot K, Mesters S and Lüth H 1997 *Appl. Phys. Lett.* **71** 410
Gossmann H J and Fisanick G J 1990 *Scanning Microsc.* **4** 543
Gray L J, Chrisholm M F and Kaplan T 1995 *Appl. Phys. Lett.* **66** 1924
Hartmann A, Vescan L, Dieker C, Stoica T and Lüth H 1993 *Phys. Rev.* B **48** 18 276
Jacobi K 1999 Substrate preparation for thin film deposition *Handbook of Thin Film Process Technology Part G2,* ed D A Glocker and S I Shah (Bristol: Institute of Physics Publishing) p G2:1
Jin G, Tang Y S, Liu J L, Thomas S G and Wang K L 1999 *Semiconductor Quantum Dots (MRS Symp. Proc. vol 571)* ed S C Moss *et al* (Warrendale, PA: Materials Research Society) p 31
Kamins T I, Carr E C, Williams R S and Rosner S J 1997 *J. Appl. Phys.* **81** 211
Kamins T I and Williams R S 1997 *Appl. Phys. Lett.* **71** 1201
Kamins T I, Williams R S and Basile D P 1999 *Nanotechnology* **10** 117
Kim E S, Usami N and Shiraki Y 1999 *Appl. Phys. Lett.* **72** 1618
Koduwely H M and Zangwill A 1999 *Phys. Rev.* B **60** R2204
LeGoues F K, Hammar M, Reuter M C and Tromp R M 1996 *Surf. Sci.* **349** 249
Liu C P, Gibson J M, Cahill D G, Kamins T I, Basile D P and Williams R S 2000 *Phys. Rev. Lett.* **84** 1958
Marée P M J, Nakagawa K, Mulders F M, Van de Veen J F and Kavanagh K L 1987 *Surf. Sci.* **191** 305
Medeiros-Ribeiro G, Kamins T I, Ohlberg D A A and Williams R S 1998 *Phys. Rev.* B **58** 3533
Miyao M, Nakagawa Y, Kimura Y and Hirao M 1998 *J. Vac. Sci. Technol.* B **16** 1529
Mo Y M, Kleiner J, Webb M B and Lagally M G 1992 *Surf. Sci.* **268** 275
Mo Y-W, Savage D E, Swartzentruber B S and Lagally M G 1990 *Phys. Rev. Lett.* **65** 1020
Osten H J, Zeindl H P and Bugiel E 1994 *J. Cryst. Growth* **143** 194
Rai-Choudhury P and Schroder D K 1973 *J. Electrochem. Soc.* **120** 664
Ratsch C and Zangwill A 1993 *Surf. Sci.* **293** 123
Ross F M, Tersoff J and Tromp R M 1998 *Phys. Rev. Lett.* **80** 984
Sanguinetti S, Chiantoni G, Grilli E, Guzzi M, Henini M, Polimeni A, Patan A, Eaves L and Main P C 1999 *Europhys. Lett.* **47** 701
Schittenhelm P, Gail M, Brunner J, Nützel J F and Abstreiter G 1995 *Appl. Phys. Lett.* **67** 1292
Schmidbauer M, Wiebach Th, Raidt H, Hanke M, Köhler R and Wawra H 1998 *Phys. Rev.* B **58** 10 523
Shchukin V A, Ledentsov N N and Kop'ev P S 1995 *Phys. Rev. Lett.* **75** 2968

Shklyaev A A, Shibata M and Ichikawa M 1999 *Surf. Sci.* **416** 192
Spencer B I and Tersoff J 1997 *Phys. Rev. Lett.* **79** 4858
Stoica T 2001 unpublished
Stoica T 2002 to be submitted
Sullivan J S, Evans H, Savage D E, Wilson M R and Lagally M G 1999 *J. Electron. Mater.* **28** 426
Sunamura H, Usami N, Shiraki Y and Fukatsu S 1995 *Appl. Phys. Lett.* **66** 3024
Sutter P, Mateeva E and Lagally M G 1998 *J. Vac. Sci. Technol.* B **16** 1560
Tersoff J 1991 *Phys. Rev.* **43** 9377
Tersoff J and LeGoues F K 1994 *Phys. Rev. Lett.* **72** 3570
Tersoff J, Teichert C and Lagally M G 1996 *Phys. Rev. Lett.* **76** 1675
Tersoff J and Tromp R M 1993 *Phys. Rev. Lett.* **70** 2782
Tillmann K, Jäger W, Rahmati B, Trinkhaus H, Vescan L and Urban K 2000 *Phil. Mag.* A **80** 255
Vescan L 1998 *J. Cryst. Growth* **194** 173
Vescan L, Dieker C, Souifi A and Stoica T 1997 *J. Appl. Phys.* **81** 6709
Vescan L, Grimm K and Dieker C 1998 *J. Vac. Sci. Technol.* B **16** 1549
Vescan L, Grimm K, Goryll M and Holländer B 2000a *Mater. Sci. Eng.* B **69–70** 324
Vescan L, Goryll M, Stoica T, Gartner P, Grimm K, Chretien O, Mateeva E, Dieker C and Holländer B 2000b *Appl. Phys.* A **71** 423
Vescan L, Jäger W, Dieker C, Schmidt K and Lüth H 1992 *MRS Symp. Proc.* 263 (Warrendale, PA: Materials Research Society) p 23
Vescan L and Stoica T 2002 *J. Appl. Phys.* **91** 10 119
Vescan L, Stoica T, Chretien O, Goryll M, Mateeva E and Mück A 2000c *J. Appl. Phys.* **87** 7275
Vescan L, Stoica T and Holländer B 2002 *Mater. Sci. Eng.* B **89** 49
Voigtländer B and Zinner A 1993 *Appl. Phys. Lett.* **63** 3055
Walz J, Greuer A, Wedler G, Hesjedal T, Chilla E and Koch R 1998 *Appl. Phys. Lett.* **73** 2579
Weil J D, Deng X and Krishnamurthy M 1998 *J. Appl. Phys.* **83** 212
Zhang 1999 *Appl. Phys. Lett.* **75** 205
Zhu J, Miesner C, Brunner K and Abstreiter G 1999 *Appl. Phys. Lett.* **75** 2395
Zinke-Allmang M 1992 *J. Vac. Sci. Technol.* B **10** 1984
Zinke-Allmang M 1999 *Thin Solid Films* **346** 1
Zinke-Allmang M and Stoyanov S 1990 *Japan. J. Appl. Phys.* **29** L1884